

POLYMER MAGNETIC SCANNER

Olgaç Ergeneman, Arda D. Yalçınkaya, Melih Altun, Rifat Türsen, Hakan Urey
 Koç University, Electrical Engineering Rumelifeneri Yolu TR-34450 Istanbul, Turkey
 hurey@ku.edu.tr

Abstract — A polymer based 1-D electromagnetic scanner is developed for barcode reading applications. The system consists of a mirror suspended by a polymer cantilever beam, a permalloy sheet placed under the mirror, and a coil to generate the driving magnetic field. Modeling of the device using analytical methods and finite element analysis are presented along with the experimental results. This work focuses on small-angle magnetic actuation of the scanner; the effects of coil parameters on the material magnetization and the hysteresis of the magnetic force on the scanner dynamics are discussed. A barcode reading system is demonstrated successfully using this inexpensive, easily manufacturable scanner.

Key Words: Magnetic actuation, permalloy, barcode

I INTRODUCTION

Scanning mirrors and rotating prisms are used in barcode reading systems to scan the laser beam over the barcode surface. Development of polymer scanners is driven by the need for inexpensive, compact, low resonant frequency and easily manufacturable scanners for barcode reading and other imaging applications. An electromagnet and a polymer scanner with magnetic material can be utilized to achieve a system with the desired properties. Silicon microactuators for other applications are presented in a number of papers [1-5]. Using soft materials such as polymer enables low resonant frequency scanners that eliminate the need of fast electronics for signal processing. Furthermore mold shaping of polymers reduces manufacturing costs yielding low cost scanners.

II ACTUATOR DESIGN

II.1 STRUCTURE OF THE SCANNER

Polymer resin (RenShape SL5195) was molded and cured by UV light into the desired scanner shape. Mold defines both the flexure and the mirror dimensions. As illustrated in Fig. 1, the cantilever beam is anchored from the left and the rectangular plate at the right supports the mirror and the magnetic material. A silicon wafer is coated with Aluminum and diced into square pieces and attached to the polymer plate from the top and the

electroplated magnetic material (NiFe – permalloy) is attached to the bottom side of the plate. The plate is suspended by a cantilever beam designed to allow out-of-plane deflections. An electromagnet is placed under the magnetic material to generate the driving magnetic field, $H_{applied}$.

II.2 THEORY OF OPERATION

The deflection of the scanner is modeled using the balance between the magnetic torque T_{mag} and the mechanical restoring torque T_{mech} . The magnetic torque T_{mag} , generated by the interaction of the permalloy sheet and the external magnetic field is given by [2,5]

$$T_{mag} = V_p M_p H_{applied} \sin(\phi - \theta) \quad (1)$$

where V_p is the volume of permalloy, M_p is the magnetization of the permalloy induced by the parallel component of $H_{applied}$, ϕ is the angle between $H_{applied}$ and the initial direction of M_p

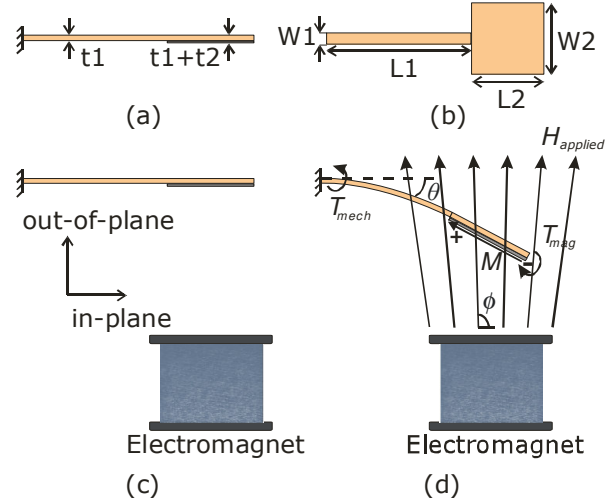


Figure 1. Schematic representation of the magnetic actuator. (a) Side view and (b) top view of the cantilever beam scanner. Overall thickness is 0.5 mm and rectangular mirror is 8x8 mm, flexure dimensions adjusted to meet different frequencies. (c) Rest position of the scanner when $H_{applied}$ equals zero. (d) Out-of-plane deflection when $H_{applied}$ provided by an electromagnet is greater than zero.

and θ is the deflection angle of the scanner. The deflection angle of the scanner for small deflections is given by [2]

$$\theta = -\frac{T_{mech}}{k_s} \quad (2)$$

where k_s is the stiffness of the suspension beam, calculated through the Young's modulus of the polymer and the geometry of the spring. The moment of inertia of the mirror is much greater than the moment of inertia of the suspension beam; therefore the bending of the mirror is negligible and is not considered in this paper. This assumption is verified with FEM simulations. Density and the Young's modulus for the material used are 1180 kg/m^3 and 1628 MPa .

The regime of large angular displacement has been studied in a number of papers [2-4]. This paper focuses on the permalloy actuator's small-angle rotations. The magnetization of the permalloy sheet is assumed to remain along the easy axis which is parallel to the surface caused by the high shape magnetic-anisotropy [2]. The out-of-plane component of the magnetic field is not sufficient to magnetize the permalloy sheet for small angular displacements.

III EXPERIMENTAL RESULTS

Cantilever beam scanners with various flexure and rectangular plate dimensions were fabricated to obtain different frequencies. The effect of the in-plane component of the magnetic field on the magnetization hence to the angular displacement, is observed by using a large coil with 68 mm outer diameter and 60 mm length incorporating an 16 mm diameter magnetic core at its center.

The magnetic field simulations are performed using finite element modeling software (FEMLAB 3.1). Fig. 2 shows the in-plane (H_r) and out-of-plane (H_z) components of the magnetic field versus the distance between the coil and the permalloy sheet. Fig. 3 shows the product of H_r and H_z as the electromagnetic torque depends on the $M_p H_z$ product and M_p is a nearly linear function of H_r . From Fig. 3 the maximum torque can be achieved by placing the permalloy sheet about 3.5 mm from the coil. Also the product increases going away from the center axis. Fig. 4 shows the experimental

peak-to-peak deflection of the scanner placed around the center of the coil as a function of the distance between the coil and permalloy which is consistent with the FEM simulations. The coil was excited with a biased-sinusoidal current waveform at the scanner's resonant frequency of 49 Hz.

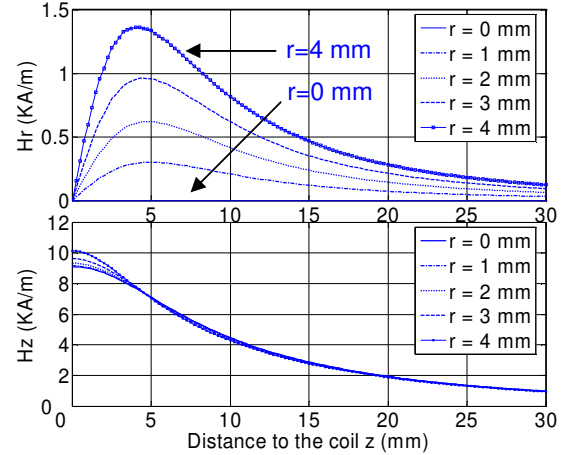


Figure 2. FEM simulations of the in-plane, H_r and out-of-plane, H_z component of the magnetic field $H_{applied}$ plotted versus distance between the coil and permalloy sheet taken at different radial distances from the central axis.

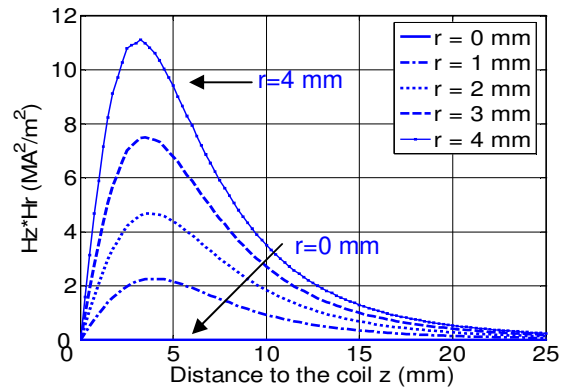


Figure 3. FEM simulations of the product of H_r and H_z versus the distance between the coil and the permalloy sheet.

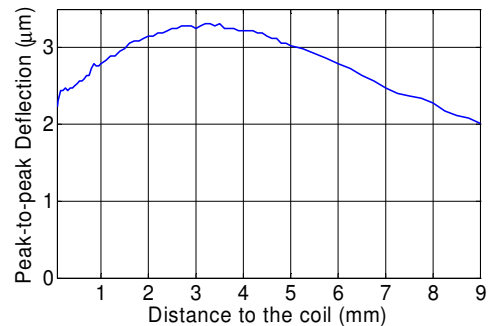


Figure 4. Peak-to-peak deflection of the scanner versus the distance between the coil and the permalloy sheet.

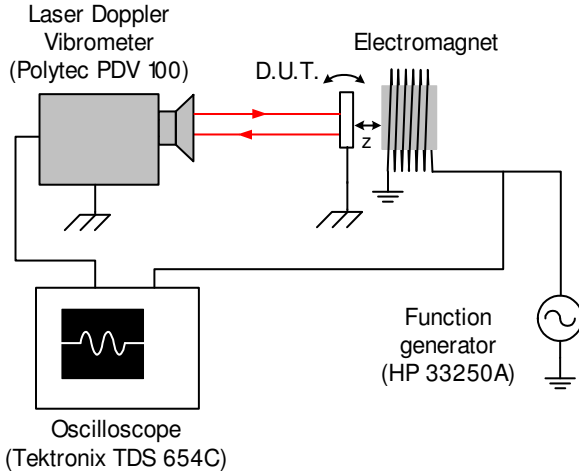


Figure 5. The characterization setup used for extracting dynamic behavior of the polymer scanner.

The dynamic deflection of the scanner was measured using a laser Doppler vibrometer (LDV) (Fig. 5). Fig. 6 shows the peak-to-peak deflection of the scanner when an ac signal on top of a dc offset is applied. Out-of-plane flux density of 3.5 mT is generated by the dc current. Dc field magnetizes the permalloy sheet and ac signal results in oscillation at the scanner resonant frequency. The difference between theory and experimental data at high ac currents originates from the change in magnetization, which is kept constant at its dc value in the theoretical calculations.

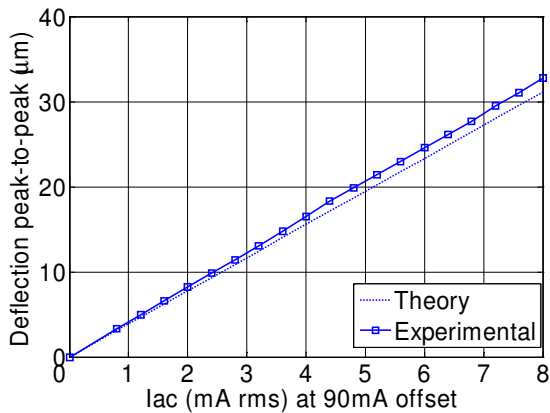


Figure 6. Tip deflection as a function of the ac drive current on top of a 90 mA DC current applied to a 1200 turn coil.

Fig. 7 shows the frequency response of the scanner for different offset values. Fig. 8 shows the frequency response of the scanner for different coil distances. As the distance is decreased, a slight spring softening effect is observed due to larger deflections.

Fig. 9 shows the peak-to-peak deflection of the scanner as a function of the offset voltage in order to show the dependency of the scanner deflection to the offset magnetic field.

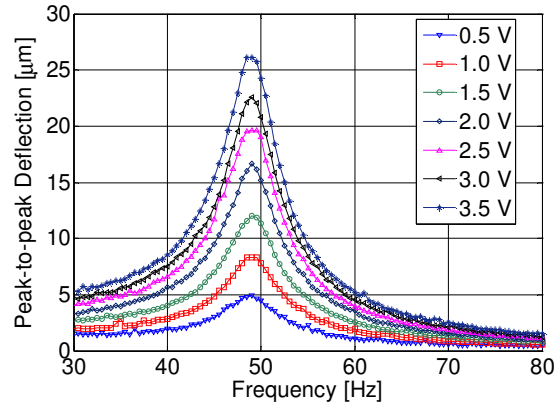


Figure 7. Offset voltage dependency of the scanner resonance.

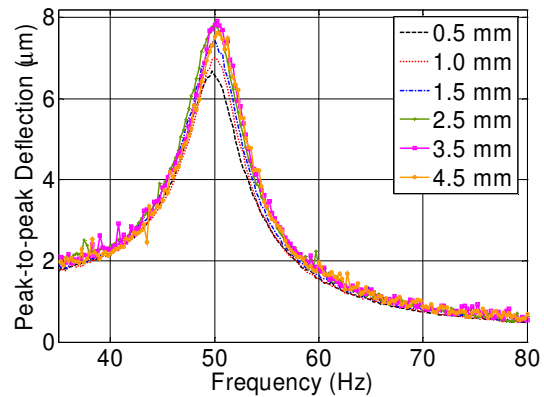


Figure 8. Dependency of the scanner resonance to the distance between the scanner and the coil.

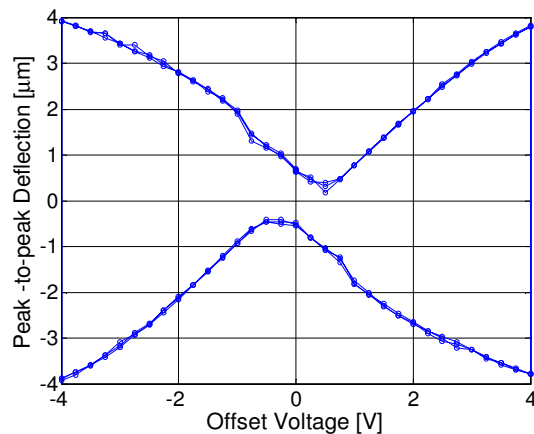


Figure 9. Peak-to-peak deflection of the scanner as a function of the offset voltage. The positive and negative values are used to indicate direction.

The deflection is plotted positive for forward sweep of the offset voltage and plotted as negative for backward sweep of the bias voltage. Nonlinearity and the hysteresis in the curve is due to the typical BH curve of the materials. The minimum ac deflection is attained at a non-zero value of the offset, which is due to the magnetization that remains on the scanner even when the field is zero.

IV BARCODE APPLICATION

The scanner explained in this paper is used in a barcode reader system. A smaller coil is used to actuate the scanner and generate high in-plane and out-of-plane magnetic fields. The coil is driven with a sinusoidal signal on a DC offset at the mechanical resonance of the scanner and mechanical deflections of ± 5 degrees were observed. The schematic representation of the system is illustrated in Fig. 10. Light from a laser diode is incident on the scanner. The light is focused and scanned over the barcode with the necessary optical elements. The scattered light is collected with a lens to the photo diode (PD) while the beam is scanned over the barcode. The output of the photo diode is processed with the necessary electronics to get the desired signal. Low resonant frequency of the scanner allowed using low-cost, widely available electronic components for data processing. Using this test setup, different kinds of barcodes are read successfully. Output of the photo diode on the scope is shown in Fig. 11. The scope output is filtered then digitized and processed with a microprocessor. Different width black and white stripes in the original barcode are reconstructed using the distance between subsequent peaks in the scope signal.

V CONCLUSION

An inexpensive, low resonant frequency polymer barcode scanner using magnetic permalloy actuator has been successfully developed. Magnetic force is maximized by optimizing the coil and scanner geometries. Resonant operation of the scanner allows filtering out the nonlinearities and hysteresis in the excitation torque, which is inherent in this type of magnetic actuator. Its operation under small deflection angles has been studied and modeled. The use of such a scanner in a barcode reading system has been demonstrated. Scanners with

smaller dimensions and similar structural materials can be utilized for better performance. The long term durability of the polymer scanner must be studied further.

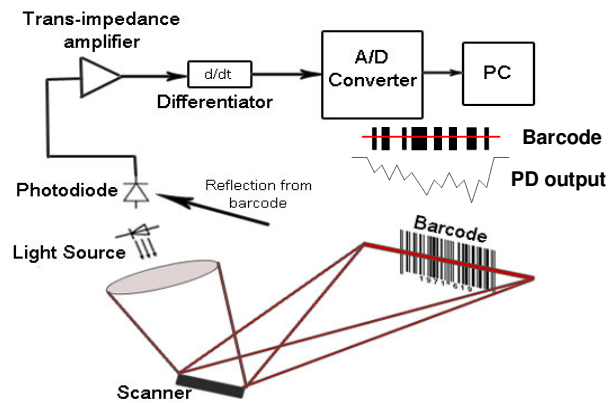


Figure 10. Schematic representation of the barcode reading system.

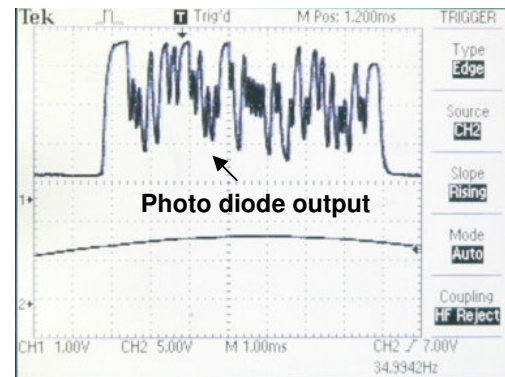


Figure 11. Output of the photo diode. Valleys are black stripes.

REFERENCES

- [1] B. Wagner, M. Kreutzer, W. Benecke, Electromagnetic microactuators with multiple degrees of freedom, *Proc. 6th Int. Conf. Solid-State Sensors and Actuators (Transducers '91) San Francisco, CA, USA*, pp 614-617, 1991
- [2] J. Judy, R. S. Muller, Magnetically actuated, addressable microstructures, *Journal of MEMS*, vol 6, no. 3, pp 249-256, 1997.
- [3] C. Liu, Micromachined magnetic actuators using electroplated permalloy, *IEEE Transactions on Magnetics*, vol. 35, no. 3, pp 1976-1985, 1999.
- [4] C. Liu, T. Tsao, G. Lee, J. T. S. Leu, Y. W. Yi, Y. Tai, C. Ho, Out-of-plane magnetic actuators with electroplated permalloy for fluid dynamics control, *Sensors and Actuators*, vol 78, pp 190-197, 1999.
- [5] R.A. Miller, G.W. Burr, Y. Tai, D. Psaltis, Electromagnetic MEMS scanning mirrors for holographic data storage, *Proc. Solid-State Sensor and Actuator Workshop, Hilton Head Island*, pp 183-186, 1996.